JOURNAL OF VIROLOGY, Nov. 2007, p. 12619–12629 Vol. 81, No. 22
0022-538X/07/$08.00+0 doi:10.1128/JVI.01017-07

Selection and Analysis of Mutations in an Encephalomyocarditis Virus Internal Ribosome Entry Site That Improve the Efficiency of a Bicistronic Flavivirus Construct[▽]

Klaus K. Orlinger, Regina M. Kofler, Franz X. Heinz, Verena M. Hoenninger, and Christian W. Mandl*

Clinical Institute of Virology, Medical University of Vienna, Vienna, Austria

Received 10 May 2007/Accepted 23 August 2007

Flaviviruses have a positive-stranded RNA genome, which simultaneously serves as an mRNA for translation of the viral proteins. All of the structural and nonstructural proteins are translated from a cap-dependent cistron as a single polyprotein precursor. In an earlier study (K. K. Orlinger, V. M. Hoenninger, R. M. Kofler, and C. W. Mandl, J. Virol. 80:12197–12208, 2006), it was demonstrated that an artificial bicistronic flavivirus genome, TBEV-bc, in which the region coding for the viral surface glycoproteins prM and E from tick-borne encephalitis virus (TBEV) had been removed from its natural context and inserted into the 3′ noncoding region under the control of an internal ribosome entry site (IRES) from encephalomyocarditis virus (EMCV) produces viable, infectious virus when cells are transfected with this RNA. The rates of RNA replication and infectious particle formation were significantly lower with TBEV-bc, however, than with wild-type TBEV. In this study, we have identified two types of mutations, selected by passage in BHK-21 cells, that enhance the growth properties of TBEV-bc. The first type occurred in the E protein, and these most likely increase the affinity of the virus for heparan sulfate on the cell surface. The second type occurred in the inserted EMCV IRES, in the oligo(A) loop of the J-K stem-loop structure, a binding site for the eukaryotic translation initiation factor 4G. These included single-nucleotide substitutions as well as insertions of additional adenines in this loop. An A-to-C substitution in the oligo(A) loop decreased the efficiency of the IRES itself but nevertheless resulted in improved rates of virus particle formation and overall replication efficiency. These results demonstrate the need for proper balance in the competition for free template RNA between the viral RNA replication machinery and the cellular translation machinery at the two different start sites and also identify specific target sites for the improvement of bicistronic flavivirus expression vectors.

Flaviviruses are small, enveloped, positive-stranded RNA viruses belonging to the genus *Flavivirus*, family *Flaviviridae*. This genus comprises several important arthropod-borne human pathogens, including yellow fever virus, West Nile virus, Japanese encephalitis virus, dengue virus, and tick-borne encephalitis virus (TBEV) (23).

Mature flavivirus virions contain only three structural proteins. The capsid protein C associates with the viral genomic RNA to form the nucleocapsid, which is enveloped by a membrane into which the two surface proteins, E (envelope protein) and M (membrane protein), are embedded (23). Virions are assembled intracellularly in an immature form containing a larger glycoprotein precursor of the M protein, called prM. Cleavage of the precursor by a cellular protease activates viral entry functions and is required for infectivity (5, 38).

The flavivirus genome is a single-stranded RNA molecule that functions as an mRNA for translation and is therefore infectious when introduced into the cell cytoplasm by transfection (35). This RNA is approximately 11 kilobases in length and has a 5′ cap structure, but it lacks a poly(A) tail at the 3′ end (42, 43). All of the viral structural and nonstructural proteins are encoded within a single open reading frame and are processed co- and posttranslationally to form the mature products.

Despite the fact that the flavivirus genome contains only a single cap-dependent translation initiation site, several studies have demonstrated that it is possible, by introducing a heterologous viral internal ribosome entry site (IRES) into the 3′ noncoding region (3′NCR), to achieve expression from a separate, cap-independent cistron, thus making it feasible to use modified flaviviruses as bicistronic expression systems for foreign genes (7, 10, 16, 18, 24, 32, 34, 36, 37, 39, 40, 44). However, many of these have been found to be unstable or inefficient and therefore need to be further developed and optimized (7, 16, 18, 32, 37).

Taking the bicistronic approach a step further, we have recently demonstrated that it is possible to engineer viable flaviviruses in which the envelope glycoproteins prM and E are expressed from a separate translation unit, driven by a foreign IRES element, instead of as part of the natural cap-dependent polyprotein (32). The bicistronic flavivirus clone was made by replacing a variable region in the 3′NCR of TBEV with a modified IRES from encephalomyocarditis virus (EMCV), removing the portion of the genome encoding prM and E from its natural position and inserting it into the 3′NCR behind the IRES. This construct, called TBEV-bc (for bicistronic TBEV), was able to replicate, to make functional infectious virus particles, and to be propagated in cell culture and in animals.

* Corresponding author. Mailing address: Clinical Institute of Virology, Medical University of Vienna, Kinderspitalgasse 15, A-1095 Vienna, Austria. Phone: 43-1-40490, ext. 79502. Fax: 43-1-40490-9795. E-mail: christian.mandl@meduniwien.ac.at.

▽ Published ahead of print on 12 September 2007.

However, TBEV-bc was significantly impaired in comparison to wild-type TBEV (TBEV-wt), and in this genomic context, the prM and E proteins were expressed rather inefficiently from the IRES cistron. However, in the same study it was also observed that viral titers sometimes increased significantly upon repeated passage of TBEV-bc virus in BHK-21 cells, suggesting that spontaneous mutations that improved the overall efficiency of the system were being selected.

Because of the considerable practical importance of improving the efficiency of the bicistronic TBEV and for understanding which elements of the flavivirus genome are of importance for the application of these viruses as expression vectors, we continued, in this study, to investigate the nature of mutations that allow these artificial genomes to better adapt to this altered arrangement and mode of expression. We found that two types of mutations are selected when TBEV-bc is passaged in BHK-21 cells. The first type involves surface amino acids in the envelope protein E that are likely to be involved in binding to cell surface glycosaminoglycans, as has been observed previously in other contexts (8, 9, 29; reviewed in reference 25). The second type, more interestingly, involves changes within the foreign IRES element. Although all of the IRES mutations actually reduced the translation efficiency of the IRES itself, some of them nevertheless improved the overall efficiency of virus replication in this system, resulting in an increase in the total amount of protein expressed from the natural cap cistron and, in some cases, from the IRES cistron as well. These mutations are therefore apparently able to compensate for the deleterious effect on virus replication that had been caused by inserting the IRES into the 3′NCR and rearranging the natural gene order, but at the same time, they preserved IRES function at a level sufficient for expressing the surface proteins in the amounts needed for virus propagation.

MATERIALS AND METHODS

Virus and cells. All of the viruses and genomic constructs used in this study were based on the TBEV prototype strain Neudoerfl (GenBank accession number U27495), and an infectious clone of this strain (27) was used as the monocistronic wild-type control in all experiments.

BHK-21 cells (ATCC CCL10) were grown at 37°C with 5% CO_2 in Eagle's minimal essential medium (Sigma) supplemented with 5% fetal calf serum (FCS), 1% glutamine, and 0.5% neomycin. After transfection, the growth medium was replaced by a maintenance medium consisting of minimal essential medium with the FCS concentration lowered to 1% and buffered with 15 mM HEPES.

COS-1 cells (ATCC CRL 1650) were grown at 37°C with 5% CO_2 in Dulbecco's modified Eagle medium containing 10% FCS, 4 mM glutamine, 100 U penicillin, and 100 μg streptomycin per ml. After transfection, the medium was replaced with the same medium with the FCS concentration reduced to 1%.

Infectious RNA synthesis and cell transfection. Infectious genome-length RNA was synthesized by in vitro transcription as described previously (27), using plasmid clones derived from either pTNd/c (27) or pTNd/bc (32) as templates. After the transcription reaction, the template DNA was digested with DNase I and the RNA was purified using an RNeasy minikit (QIAGEN). The integrity of the RNA was checked by electrophoresis in a 1% agarose gel containing 6% formalin. RNA was quantitated spectrophotometrically (19), and equal amounts of RNA were used for all transfections. BHK-21 cells were transfected by electroporation using a Bio-Rad GenePulser apparatus as described previously (7, 27).

Virus titration. Supernatants of infected or RNA-transfected cells were sequentially diluted in either $\log_{10}$ or 0.5 $\log_{10}$ steps, depending on the experiment, and 200 μl of each dilution was applied to fresh BHK-21 cells grown on coverslips in a 24-well cluster plate. Three days later, cells were fixed and permeabilized, and an indirect immunofluorescence assay was carried out as described previously using a polyclonal rabbit antiserum (32). The endpoint dilution was defined as the last dilution at which positive fluorescent cells were detected.

Selection of mutants. BHK-21 cells were transfected by electroporation with the appropriate in vitro-synthesized RNA and distributed into individual wells of a 24-well plate. In parallel, transfected cells were transferred to a plate containing glass coverslips, and these cells were examined at 3 days posttransfection by the immunofluorescence assay to check the transfection efficiency. After 16 h, the cells were washed twice with 0.5 ml of maintenance medium per well and then allowed to grow in 1 ml of maintenance medium for another 6 days, after which the supernatants were collected and cleared by low-speed centrifugation at 4°C. A 0.2-ml aliquot of the cleared supernatant was then used to inoculate fresh BHK-21 cells in another 24-well plate, and the remainder was frozen at −80°C and used later for virus titration and RNA quantitation. After 90 min, the inoculum was removed, the cells were washed twice as described above, and these cells were likewise allowed to grow for 6 days in 1 ml of fresh medium. This procedure was repeated a total of six times with supernatants from all wells in which the cells displayed an altered morphology, which preliminary experiments had shown to be indicative of an increase in infectivity, and the infectious titers of these samples were determined after each passage using the endpoint titration assay.

Cell supernatants containing variants that had exhibited a significant increase in virus titer during the sequential passaging steps were then used to infect fresh BHK-21 cells in 25-cm^2 tissue culture flasks. These infected cells were harvested by trypsinization at 4 days after infection, and cytoplasmic RNA was isolated using an RNeasy minikit (QIAGEN). This RNA was reversed transcribed using a cDNA synthesis kit (Roche) and amplified by PCR. DNA sequences were determined using a automated sequencing system (PE Applied Biosystems, model 3100 or 310).

Cloning procedures. The construction and characterization of the full-length plasmid clone, pTNd/bc, which was used to generate the bicistronic RNA genome of TBEV-bc and its derivatives was described in a previous study (32). The genomic RNA generated from this construct lacks the region encoding the prM and E proteins in the open reading frame encoding the viral polyprotein but retains the portions encoding the capsid protein and all of the viral nonstructural proteins in the natural cap-dependent cistron. A modified EMCV IRES inserted into a variable region of the 3′NCR followed by the region encoding the prM and E glycoproteins allows separate expression of these proteins. The IRES was derived from the commercially available vector pIRES2-eGFP (Clontech), which includes nucleotides 260 to 848 of the EMCV genome sequence (GenBank accession number M81861) but has one additional A residue in its oligo(A) loop (i.e., there are seven A's in the Clontech vector-derived IRES, compared to six A's in the natural sequence of EMCV).

The E protein mutations D308A and A317T were introduced into TBEV-bc by exchanging a fragment encoding the C-terminal region of the E protein with the corresponding one from the mutant. This sequence was generated by PCR using a set of primers in which the 53-nucleotide-long forward primer incorporated the selected mutations as well as a recognition site for the restriction enzyme SnaBI (at position 1878 according to the numbering of the TBEV-wt genome) and the reverse primer contained an artificial stop codon and NotI site immediately after the E-coding sequence. Using SnaBI and NotI, this DNA was cloned into the corresponding site in pTNd/bc to generate the full-length construct pTBEV-bc(E-D308A+A317T).

For analysis of mutant IRES elements using the reporter assay, selected IRES variants were cloned into the commercially available expression vector pIRES2-eGFP (Clontech) using the unique restriction sites for SacII and BstXI that flank the IRES in this plasmid. cDNA from the selected variants was amplified using an Advantage-HF 2 PCR kit (BD Bioscience) with specific primers containing the appropriate restriction enzyme recognition sites, and after cutting the vector and the insert with these enzymes, these were ligated together and introduced by electrotransformation into *Escherichia coli* strain HB101 and correct clones were identified by DNA sequencing.

As an intermediate step in the introduction of IRES mutations into genome-length clones, these mutations were first introduced into pIRES2-prME, a plasmid clone containing only the region corresponding to the IRES cistron (32). pIRES2-prME constructs carrying the individual IRES mutations were assembled in three-fragment ligations consisting of (i) the fragment containing the altered IRES, excised by BstXI and SacII restriction enzymes from the appropriate pIRES2-eGFP construct (described above); (ii) BstXI- and SacII-digested pIRES2-prME vector backbone (lacking the IRES and the 5′ part of the contiguously encoded prME sequence); and (iii) the BstXI-SacII-excised fragment encoding the 5′ part of the prME coding sequence.

Full-length bicistronic clones containing a mutant IRES in an otherwise wild-type background were generated by excising the region containing the IRES,

prM, and E from the appropriate pIRES2-prME construct (described above) by digestion with SacII and SnaBI and replacing the corresponding region in pTNd/bc with this restriction fragment. To make the combined mutant with both the IRES-A771C and E-D308A-A317T mutations, a SacII/SnaBI fragment containing the mutant IRES, prM, and a portion of E upstream of the E protein mutations was removed from the corresponding pIRES2-prME construct and used to replace the corresponding fragment of pTBEV-bc(E-D308+317T), which already contained the D308 and A317T changes (described above), to generate pTBEV-bc(IRES-A771C/E-D308A+317T).

IRES reporter assay. To measure the effects of mutations on IRES function in a conventional reporter assay, using nonreplicating RNA, variants of the expression plasmid pIRES2-eGFP (Clontech) containing nucleotide changes in the IRES (described above) were introduced into COS-1 cells by electroporation and seeded in 25-cm^2 culture flasks. At 16 hours after electroporation, the cells were washed twice, and the medium was replaced with 10 ml maintenance medium containing 1% FCS. Then, at 24-h intervals after transfection, cells were detached by treatment with trypsin-EDTA (Sigma) and collected in 5 ml growth medium. Cells were pelleted by centrifugation (800 rpm, 7 min) and resuspended in 5 ml phosphate-buffered saline (PBS) containing 0.5% bovine serum albumin (BSA). After an additional centrifugation step, cells were resuspended in 1 ml PBS containing 0.5% BSA, and fluorescence was measured in a FACSCalibur flow cytometer (Becton Dickinson) (15-mW argon laser, 488 nm) with a 530/30 band-pass filter (FL-1). The main cell population was gated, and 10,000 cells were counted per sample. CellQuestPro was used to determine the fluorescence intensity of the brightest 10% of the cells, and this value was used in order to compensate for differences in electroporation efficiency.

RNA export assay. Aliquots of 140 μl of supernatant from transfected cells were cleared by low-speed centrifugation, and the viral RNA was isolated using a QIAamp viral RNA minikit (Qiagen) according to the manufacturer's instructions. Ten microliters of the isolated RNA was used as a template for cDNA synthesis using an iScript cDNA synthesis kit (Bio-Rad) according to the manufacturer's protocol. Half of this material was then used directly for quantitative real-time PCR analysis (PE Applied Biosystems) as described in an earlier publication (19). The original RNA concentration of each sample was determined using a standard curve in which serial 10-fold dilutions of an RNA preparation of known concentration were subjected to the same amplification steps as the samples.

Measurement of NS1 and E protein expression. The relative amounts of NS1 and E protein in BHK-21 cells after transfection were determined by fluorescence-activated cell sorter (FACS) analysis as described previously (32). Cells were transfected by electroporation with the appropriate genomic RNA and transferred to 25-cm^2 tissue culture flasks. The medium was replaced 20 h after transfection with maintenance medium, and cells were allowed to grow for different lengths of time until harvest. At each time point, cells were harvested by trypsinization and washed three times in PBS containing 2% BSA. Cells were then counted in a Casy TT cell counter (Schärfe Systems), and 200,000 cells were fixed and permeabilized using the provided Lysing and Perm2 solutions (BD) diluted 1:10 in PBS. After each reaction, cells were washed twice with PBS containing 0.5% BSA. After permeabilization, cells were split into two halves and incubated for 30 min at 37°C with either a monoclonal anti-E antibody (B2) (11) or a monoclonal anti-NS1 antibody (6E11) (15), followed by two consecutive washing steps. Cells were then stained with fluorescein isothiocyanate-conjugated anti-mouse antibodies (Jackson Immunoresearch Laboratories) for 30 min at 37°C. Two further washing steps served to remove nonspecifically bound antibodies, and stained cells were resuspended in 200 μl PBS containing 0.5% BSA.

A FACSCalibur flow cytometer (Becton Dickinson) (15-mW argon laser, 488 nm) with a 530/30 band-pass filter (FL-1) was used to measure the fluorescence intensity of the stained cells. The main cell population was gated and 10,000 cells counted per sample. Analysis of the samples was carried out using CellQuestPro software (Becton Dickinson). To allow for differences in RNA transfection efficiencies and virus infectivity, mean values were calculated for the 10% of the cell population that exhibited the brightest fluorescence intensity (rather than using the entire cell population, which could contain different percentages of positive cells in different samples).

RESULTS

Selection of adaptive mutations in BHK-21 cells. The altered genetic organization of the artificial bicistronic TBEV construct, TBEV-bc, is shown in comparison to the normal, monocistronic TBEV-wt genome in Fig. 1A. In TBEV-bc, the prM and E glycoproteins are no longer expressed as part of the normal cap-dependent cistron at the 5′ end of the genome, but instead, this region is translated separately under the control of an inserted EMCV IRES element at the 3′ end of the genome. All of the other viral proteins, i.e., capsid protein (C) and the viral nonstructural proteins (NS1 to NS5), are still translated as part of the original cap cistron. This altered genome arrangement yields viruses that are viable but replicate considerably less efficiently than wild-type virus (32).

In order to establish a basis for optimizing the efficiency of bicistronic flavivirus vectors, we attempted to generate adaptive mutations in TBEV-bc by repeated passage in cell culture. This was done by transfecting BHK-21 cells with in vitro-synthesized full-length genomic TBEV-bc RNA, collecting the cell supernatant 6 days later, and then using this supernatant as the initial inoculum for multiple cycles of serial passage in fresh BHK-21 cells. An equal amount of infectious RNA from a TBEV-wt clone was used as a control.

In the initial passage experiments it was observed that the cells in approximately 20% of the wells had a visibly altered cell morphology (cell rounding, shrinking, and detachment) that was already noticeable after the first passage and was quite pronounced after the second passage. Titration of the cell supernatants revealed that the infectious titers in these wells had increased, but they had not increased in the ones in which the appearance of the cells had not changed (data not shown). Therefore, in subsequent experiments, visual screening was used as the first step in identifying potential mutants.

The results of a representative passage experiment are shown in Fig. 2. The figure shows that repeated passage of TBEV-bc resulted in sequential increases in infectious titer, indicating that variants were being selected. The endpoint titers generally increased from about 10^1 to 10^2 in the first passage to about 10^5 in the sixth passage. The titer of the monocistronic wild-type control increased from about 10^5 to 10^7 after the first passage and then remained constant after that.

To identify which mutations had been selected, supernatants from the sixth passages of different independent passaging experiments were used to infect fresh BHK-21 cells, and viral RNA was collected from the cytoplasm of these cells and reverse transcribed into cDNA. After PCR amplification, nucleotide sequencing revealed that these mutants contained nucleotide changes at two separate loci: (i) point mutations resulting in amino acid changes at the surface of the envelope protein E (Table 1) and (ii) nucleotide substitutions and insertions in a limited region of the inserted IRES element (Fig. 1B). The entire genomes of two of the mutants were sequenced, and these mutants did not contain changes in any other parts of the genome, indicating that the changes in the IRES and E protein were solely responsible for the increased titers. The nucleotide sequence of the entire region containing the IRES was determined for all seven of the mutants that had been chosen for further analysis, and all seven contained at least one nucleotide change within the IRES. The E protein regions of three of these were sequenced, and substitutions resulting in amino acid changes were found in all three (Table 1).

In two separate experiments, the D308A mutation was selected together with another amino acid substitution in the E

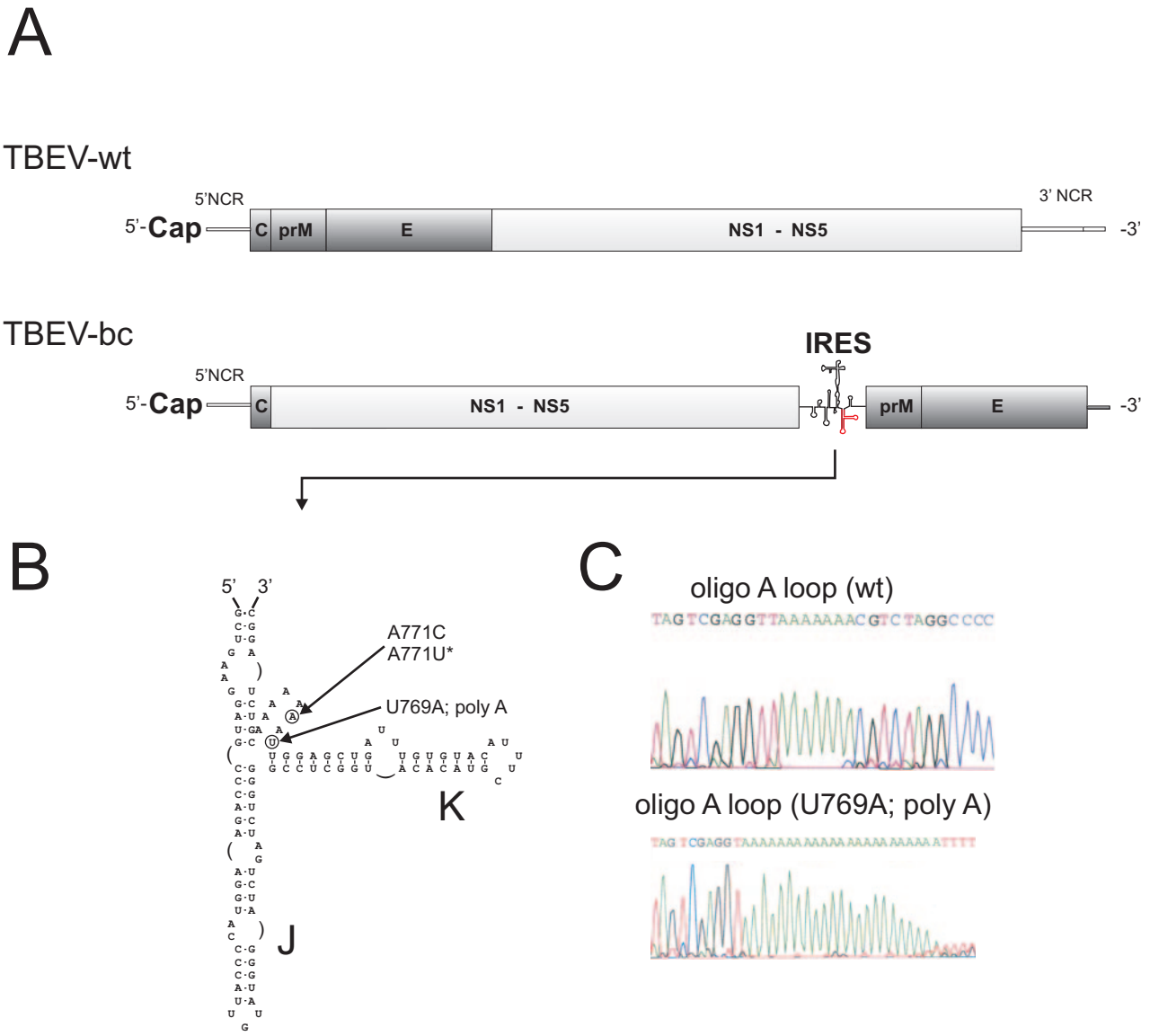

FIG. 1. TBEV-bc genome and adaptive mutations. (A) Genome organization of TBEV-wt and bicistronic TBEV-bc. The regions encoding structural proteins C, prM, and E are shown by dark gray boxes, and the regions encoding nonstructural proteins NS1 to NS5 are indicated by light gray boxes. The 5′NCR and 3′NCR are indicated. The J-K stem-loop of the EMCV IRES in TBEV-bc is colored red. (B) Sequence and secondary structure of the EMCV IRES J-K stem-loop, showing the positions of selected mutations in the oligo(A) loop region (with 7 A's as derived from the Clontech vector). The asterisk indicates a mutation that was independently isolated from mouse brain. (C) Electropherograms showing the sequences of the original oligo(A) loop and a representative U769A/poly(A) mutant with multiple adenine insertions.

protein, Ala to Thr at position 317. Although the A317T mutation did not result in a change in surface charge, the fact that neither of these mutations was selected without the other one suggests that it might stabilize the protein by compensating structurally for the D308A mutation. This explanation is supported by an earlier study in which it was found that an Asp-to-Lys mutation at position 308 was unstable unless accompanied by another stabilizing mutation (26).

Two of the three amino acid changes observed in the E protein (E387K and D308A) resulted in a net increase in the overall positive charge of the protein: a change from Glu to Lys at position 387 (resulting in the loss of one negative charge and the simultaneous gain of a positive charge) and a change from Asp to Ala at position 308 (resulting in the loss of one negative charge). It was shown previously that this type of mutation, which increases the affinity of virus binding to cell surface glycosaminoglycans (9, 22, 29), is frequently selected when the virus is adapted to growth in cell culture, and, in fact, the E387K mutation itself was selected in BHK-21 cells in an earlier study (29).

The mutations in the EMCV IRES all occurred in an important functional region, the conserved oligo(A) loop (21), which forms a bulge in the J-K stem-loop structure (Fig. 1B). This loop normally consists of five or six consecutive adenine residues in naturally occurring viral type II IRES segments (2, 12), but some IRES elements used in artificial recombinant

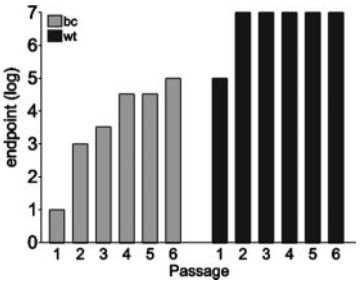

FIG. 2. Selection of variants in BHK-21 cells. (A) TBEV-bc (gray bars) and TBEV-wt (black bars) were passaged six times in cell culture, and individual endpoints were determined after each passage by limiting dilution. In the representative experiment shown here, after six passages, an A771C mutation was found in the IRES and a D308A/A317T double mutation was found in the E protein-coding region. The 100-fold increase observed for wild-type virus has been observed in previous studies and is associated with an acquired increase in affinity for heparan sulfate (29).

cDNA vectors such as pIRES2-eGFP from Clontech, which was the source of the IRES used for our constructs, have seven A residues. The oligo(A) loop is directly involved in binding the eukaryotic translation initiation factor 4G (eIF4G), therefore playing a critical role in cap-independent translation (20, 21). One of the selected mutations was an A-to-C change at the position in the IRES corresponding to nucleotide 771 of the EMCV genome (GenBank accession no. M81861), which is the second of seven A's in the loop of the Clontech IRES (Fig. 1B).

Another group of mutations, U769A/poly(A), resulted in a change in the last U preceding the loop to an A, accompanied by the insertion of multiple adenine residues into the loop (Fig. 1C). Direct sequencing of the cDNA showed that the number of A's was variable within the RNA population, resulting in a mixture of lengths. By subcloning this region into a pIRES2-eGFP expression vector and sequencing 10 different clones, it was found that the number of additional A's added to the loop ranged from 11 to 37, thus increasing the original loop size from 7 A's to as many as 45 (Table 2). None of the 10 mutants was predicted by the RNA secondary structure prediction software mfold (45) to change the overall RNA fold of the IRES; they increased only the size of the oligo(A) loop (data not shown). It is likely that the population of mutants also included variants with other numbers of A's, possibly forming a continuum. Furthermore, since it is possible that at least some of the additional A's were added by slippage of *Taq* polymerase during the amplification procedure rather than by the viral polymerase during replication, we cannot conclude that a particular number of A's had actually been selected in cell culture. However, as presented later in this report, we did find that relatively large insertions of A's at this position are surprisingly well tolerated and allow viable progeny to be produced.

TABLE 1. Selected mutations in protein E

Change (position)		No. of times selected	Domain
Nucleotide[a]	Amino acid[b]		
G→A (2131)	Glu→Lys (387)	1	III
A→C (1895)[c]	Asp→Ala (308)[c]	2	III
G→A (1921)[c]	Ala→Thr (317)[c]	2	III

[a] Numbers are according to the wild-type TBEV genomic sequence (GenBank accession no. U27495).
[b] Numbers start from the amino terminus of protein E.
[c] Both of these substitutions were present in both clones.

TABLE 2. Adenine insertion mutations in the IRES oligo(A) loop

IRES	No. of inserted A residues	Nucleotide at position 769	Total no. of A residues
Wild type		U	5–6/7[a]
Mutant clones			
1	11	A	19
2	13	A	21
3	15	A	23
4	16	A	24
5	16	A	24
6	17	A	25
7	18	A	26
8	19	A	27
9	23	A	31
10	37	A	45

[a] Natural IRES sequences contain five to six A residues; the Clontech IRES used for the construction of TBEV-bc contained seven A residues.

Selection of an A771U mutation in mouse brain. In earlier work (32), we constructed a bicistronic derivative of TBEV-bc (TBEV-bcYF) in which the region coding for the second transmembrane segment of the E protein was replaced with the corresponding region from another flavivirus, yellow fever virus. Although this mutant was severely impaired and failed to cause a lethal infection in 22 of 23 suckling mice, one mouse in this experiment developed encephalitis and died. Sequence analysis, surprisingly at that time, did not reveal any amino acid changes in the E protein transmembrane domain, and the reason for this restoration of pathogenicity was therefore not identified.

However, in the light of the observations described above, we decided to reexamine this mutant to see if a change in the foreign IRES element might have been involved in its adaptation to growth in mouse brain. We therefore used primers flanking the IRES to amplify and sequence this portion of the TBEV-bcYF genome and found that it contained an A-to-U substitution at position 771 in the IRES—exactly the same nucleotide position where an A-to-C substitution had occurred in BHK-21 cell-passaged virus (Fig. 1B). Although this finding does not prove an involvement of this mutation in the expression of a more pathogenic phenotype in mice, the selection of a change at nucleotide 771 in mouse brain as well as in cell culture provides corroborating evidence that replacing the adenine residue at this position in the bicistronic genome increases viral fitness.

Effect of IRES and E protein mutations on specific infectivity and virus production. All of the mutants that were generated in BHK-21 cells contained changes in both the E protein and the IRES. Therefore, it was necessary to separate these mutations in order to study the individual effect of each one. This was done by cloning them back separately into the original TBEV-bc plasmid construct and using the new clones to make infectious RNA in vitro for transfection.

In the first set of experiments, we compared (i) TBEV-

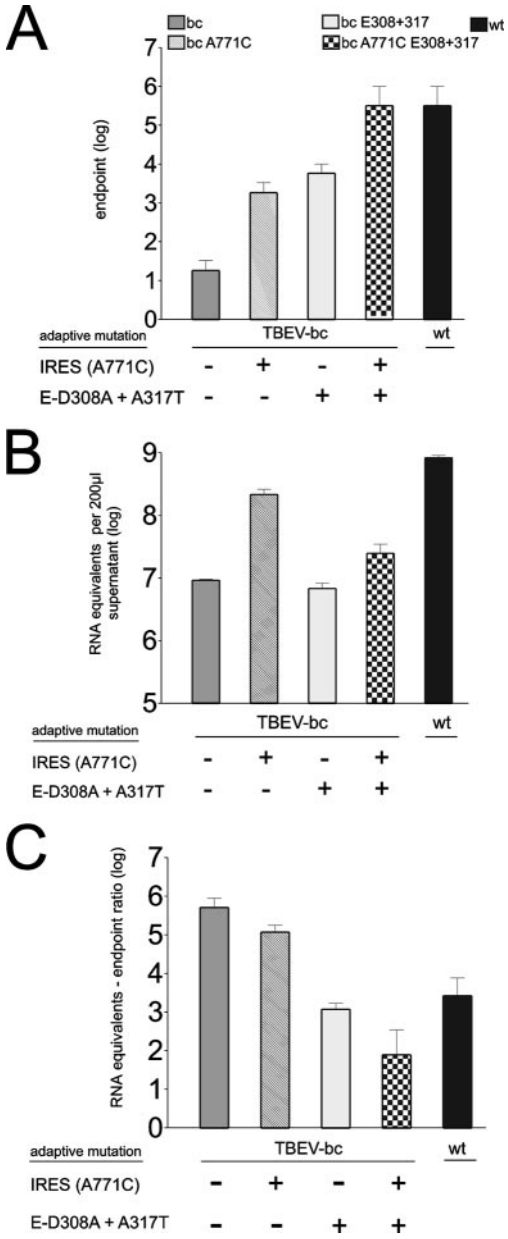

FIG. 3. Properties of TBEV-bc mutant viruses. (A) Infectivity titers of constructed mutants containing the A771C IRES mutation, the E-D308A/A317T mutation, or both, compared to TBEV-bc and TBEV-wt without mutations. Titers were determined by endpoint dilution of cell supernatants collected 6 days after transfection. (B) Quantitation of viral RNA in cell supernatant at 6 days posttransfection, determined by quantitative reverse transcription-PCR. (C) Specific infectivity of these mutants, determined by dividing the number of RNA molecules (genome equivalents) by the endpoint dilution. In all cases, the individual values are the means from two independent experiments (error bars represent the range of values).

bc(IRES-A771C), which has only a single change in the IRES; (ii) TBEV-bc(E-D308A+A317T), which was selected twice and affects a residue that is probably involved in binding to heparan sulfate; (iii) TBEV-bc(IRES-A771C/E-D308A+A317T), which is a double mutant containing both of these changes; (iv) TBEV-bc, which is the bicistronic parent construct without any adaptive mutations; and (v) TBEV-wt, the normal, monocistronic wild-type TBEV infectious clone.

Cells were transfected with equal amounts of full-length infectious RNA corresponding to each of these variants, and infectivity was determined on day 6 after transfection by the endpoint titration assay. As shown in Fig. 3A, all of the mutants had a higher infectious titer than the original bicistronic construct, and the combined mutant had a titer equal to that of the natural wild-type genome. The A771C IRES mutation by itself resulted in an approximately 2-log increase in titer; the double mutation in the E protein, D308A+A317T, resulted in a 2- to 3-log increase; and the combination of these mutations resulted in an approximately 4-log increase. This indicates that both types of mutations were advantageous for viral growth and that their effects were additive. The complementary nature of the mutations is consistent with the expectation that the IRES mutations and E protein mutations would affect completely different biological functions at different times in the viral life cycle.

The increase in viral titer could be a reflection of (i) an increase in the total number of infectious particles that were produced and released into the cell supernatant, (ii) an increase in the specific infectivity of the individual particles, or (iii) a combination of both effects. To distinguish between these possibilities, we examined the level of secretion of virus particles, by measuring the amount of viral RNA released from the cells, as well as the specific infectivity of these particles, by correlating the total amount of extracellular viral RNA with the infectious titer for each mutant.

To analyze particle secretion, BHK-21 cells were transfected with equal amounts of viral RNA, and cell supernatants were collected 6 days after transfection. The total amount of viral RNA that was released into the cell supernatants was measured by real-time PCR, and the results are shown in Fig. 3B. This experiment demonstrated that the mutations in the E protein did not by themselves significantly affect the level of virus particle formation and release, whereas both mutants containing the A771C mutation in the IRES showed higher levels of extracellular viral RNA than the unmodified TBEV-bc control. In the case of the A771C mutation by itself, the amount of RNA was about 20-fold higher than that with TBEV-bc and reached about half of the level achieved with a normal monocistronic wild-type construct. This suggests that the single nucleotide change in the IRES was responsible for an increase in the overall rate of virus particle production.

To determine the specific infectivity of the particles produced by each construct, BHK-21 cells were transfected with the appropriate viral RNA, and one aliquot of the infectious material in each cell supernatant was used to determine the titer by endpoint dilution assay, while another aliquot was used to measure the amount of genomic RNA by the real-time PCR method. This allowed the specific infectivity of each sample to be expressed as viral RNA equivalents per infectious unit by calculating the quotient of these two values.

As shown in Fig. 3C, all of the mutants displayed a decreased RNA-to-endpoint ratio relative to that for unmodified TBEV-bc, i.e., an increased specific infectivity, although the effect of the A771C IRES mutation alone was modest (five- to sevenfold). In contrast, the E protein mutant showed an almost 1,000-fold increase in specific infectivity, and the combined mutant

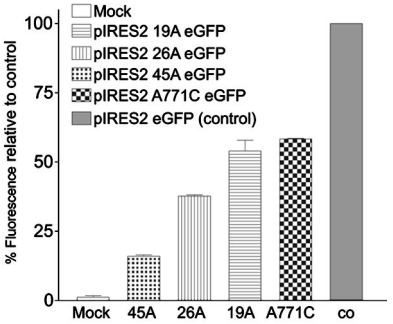

FIG. 4. Effect of mutations on eGFP expression in the IRES reporter assay. Mutant IRES elements were cloned into pIRES2-eGFP (Clontech), which served as the control (co) in this experiment. COS-1 cells were transfected by electroporation with these plasmid constructs. The relative fluorescence due to eGFP expression was measured by FACS on day 2 posttransfection. Each value is the mean from two independent experiments; error bars represent the range of values.

showed an even greater increase. These data, on one hand, are consistent with the prediction that the D308A+A317T mutation increases the specific infectivity of virus particles, probably by improving their affinity for cell surface glycosaminoglycans, and, on the other hand, suggest that the point mutation in the IRES also has a slight but significant positive effect on specific infectivity. Furthermore, because the combined mutant had the highest specific infectivity of all (in fact, higher than the wild type, which lacked a heparan sulfate-adaptive mutation), it appears that the positive effects of the mutations at these two loci are additive.

Effect of IRES mutations on reporter gene expression. Next, we wanted to take a closer look at the effect of the A771C mutation on the function of the IRES itself, i.e., its efficiency as an initiation site for translation. To do this, we introduced the A771C mutation into the reporter construct pIRES2-eGFP, which allows translation efficiency to be monitored by measuring expression of enhanced green fluorescent protein (eGFP). The mutant and parent reporter plasmids were introduced into COS-1 cells by electroporation, and cellular fluorescence due to eGFP expression was measured by FACS at 24-hour intervals for 3 days. The relative amounts of eGFP expressed on day 2 are shown in Fig. 4, where it can be seen that the modified IRES containing the A771C mutation was less efficient than the parental pIRES2-eGFP construct used as the control, with fluorescence levels reduced by 40 to 50%. This result was somewhat unexpected considering that this mutation, in the context of the bicistronic construct, had been found to have a beneficial effect on TBEV replication and clearly had given the virus a selective advantage in cell culture. On the other hand, this finding is consistent with earlier reports that other mutations in this same region have a deleterious effect on IRES function (2, 13), and the approximately twofold reduction observed here is consistent with that observed previously with an A-to-C substitution at nucleotide 772 (13, 14).

We also investigated the translation efficiency of the group of mutants that had a U769A substitution followed by the insertion of multiple A residues. For this analysis, we chose variants with 19, 26, and 45 A's in the oligo(A) loop to cover the range of insertion sizes that were found (Table 2). These mutations were subcloned into the corresponding site of the pIRES2-eGFP reporter plasmid, and the effect of the mutations on eGFP expression was investigated by FACS analysis as described above for the A771C mutant. As shown in Fig. 4, all three of these IRESs were still functional. The IRES containing 19 A's in the oligo(A) loop was still about half as strong as the parent, and remarkably, even the IRES containing 45 A's still retained about 16% efficiency. Since the level of reporter gene expression in this experiment decreased as the number of inserted A's increased, it is likely that poly(A) insertions of different lengths are tolerated at this site but impair IRES function in proportion to the size of the insert.

Influence of the A771C mutation on cap- and IRES-dependent translation in the bicistronic TBEV construct. Earlier, we showed that the IRES in TBEV-bc, although normally a powerful translation initiation element in its natural context, works rather inefficiently in its position downstream from the TBEV cap cistron. Expression of the TBEV prM and E proteins from the IRES was estimated to be 10- to 100-fold lower than when expressed as part of the normal polyprotein from the cap-dependent initiation site, and cap-dependent expression of the nonstructural protein NS1 with the bicistronic construct was also about twofold lower than with the monocistronic control (32). We therefore wanted to look at the effect of the IRES mutations generated in this study on translation efficiency in the specific context of the artificial TBEV bicistronic genome.

To assess the levels of translation from each of the cistrons, the relative amounts of proteins NS1 (from the cap cistron) and E (from the IRES cistron) were measured by FACS analysis using monoclonal antibodies. As can be seen in Fig. 5A and B, the A771C mutation, when present in the bicistronic TBEV genome, resulted in an overall increase in the levels of expression from both cistrons. Expression of NS1 from the cap cistron increased about twofold relative to TBEV-bc, restoring it to wild-type levels (Fig. 5A). At the same time, expression of E protein from the IRES cistron increased about seven to ninefold relative to TBEV-bc (Fig. 5B). This result, at first glance, is paradoxical, because the previous experiment examining reporter gene expression showed that the mutation weakens the IRES itself. Nevertheless, it is consistent with the fact that viruses containing this mutation yielded higher titers and were selected in cell culture. It thus appears that whatever disadvantage is caused by the impaired IRES function is outweighed by an overall increased efficiency of the system that is conferred by the mutation.

We then did a similar analysis of the U769A/poly(A) mutants containing 19, 26, and 45 A's by cloning them back into the TBEV-bc construct and measuring NS1 and E expression as described above. As shown in Fig. 5C, relative to TBEV-bc, all of the U769A/poly(A) mutants showed a moderate increase in expression from the cap-dependent cistron, restoring it to wild-type levels, as was also observed with the U771C mutation (Fig. 5A). This effect was the same regardless of the number of A's in the loop. In contrast, the number of A's in the IRES did have a strong effect on IRES-dependent expression of E protein, with expression levels strongly decreasing as the number of A's increased (Fig. 5D). Interestingly, these mutants showed different kinetics than the parental TBEV-bc construct, with the 19- and 26-A IRES insertion mutants producing higher

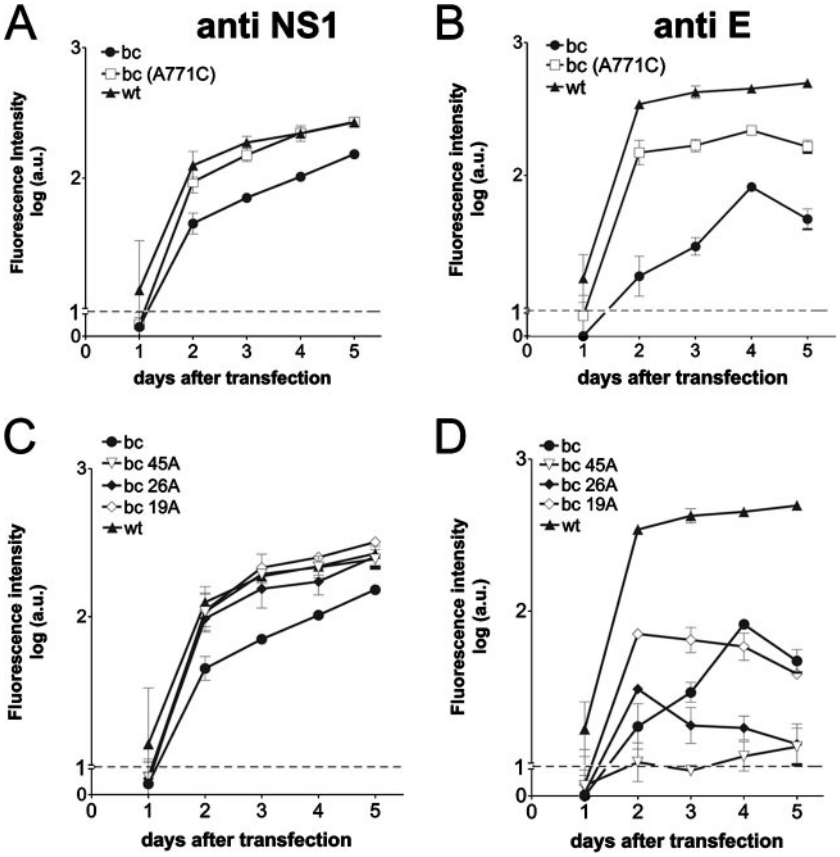

FIG. 5. Comparison of expression from the cap and IRES cistrons. On days 1 to 5 after transfection of BHK21 cells with either TBEV-bc mutant RNA or wild-type RNA, expression of protein NS1 (A and C) or envelope protein E (B and D) was determined by measuring the fluorescence intensity of cells stained using the appropriate monoclonal mouse antibody followed by a fluorescein isothiocyanate-conjugated anti-mouse antibody. The analysis of the IRES-A771C mutant is shown in panels A and B, and that of the 19-A, 26-A, and 45-A insertion mutants is shown in panels C and D. Each value is the mean from two independent experiments; error bars represent the range of values.

levels of E protein than TBEV-bc for the first 2 to 3 days, after which they were surpassed by TBEV-bc.

The infectivity and virus particle yields of the 19-, 26-, and 45-A mutants closely reflected the results from the expression experiments (data not shown). The 19-A mutant could be readily passaged, whereas the 26- and 45-A mutants were not as robust, and the 45-A construct was lost during further passage attempts. Serial passaging experiments performed with the 26-A mutant resulted in a gradual increase of viral titers, and the resulting virus population was again found to be a mixture containing adenine insertions of various lengths (data not shown). It therefore appears that large insertions in the oligo(A) loop are unstable and do not provide a long-term selective advantage. It is possible that optimal fitness of the bicistronic mutant is achieved when the virus population consists of a mixture of genomes with different numbers of A residues inserted into the oligo(A) loop.

DISCUSSION

The ability to engineer infectious flavivirus clones to accommodate expression from two separate cistrons has a number of potentially useful applications, including their use as vehicles for the expression of foreign genes as well as tools for investigating the mechanisms of virus replication and assembly (7, 10, 16, 18, 24, 32, 34, 36, 37, 39, 40, 44), but many of these systems have been hampered by poor efficiency and stability (7, 16, 18, 32, 37). We have recently shown that the ability to produce infectious, self-propagating bicistronic flaviviruses can be helpful in elucidating the details of the flavivirus replication and assembly processes by uncoupling the expression of individual proteins from the normal polyprotein processing mechanism (32), but the efficiency of this system also still requires improvement.

Here, we demonstrate that the overall efficiency of replication of the artificial bicistronic TBEV-bc was increased by repeated passage in BHK-21 cells. Flaviviruses, like most other RNA viruses, have an error-prone RNA-dependent RNA polymerase that is capable of generating frequent random mutations throughout the genome (4). This results in quasispecies in which there is usually a diverse pool of mutants from which a particular variant can be selected under the appropriate conditions (3). It is therefore interesting that the only adaptive mutations that have been observed so far in TBEV-bc were either ones in the E protein that are frequently selected in cell culture to improve cell surface binding or ones in a very limited portion of the IRES. This suggests that these two factors were the main ones limiting growth and proliferation in this system.

Earlier, it was shown that adaptation of TBEV to cell culture often involves an early selection of individual amino acid changes that increase the net positive charge of the E protein by one or two and produces a local patch of positive charge that is apparently responsible for increased affinity for heparan sulfate (22, 29). Once one of these mutations has been selected, however, further mutations of this type are not usually observed in the same virus, suggesting that increasing the positive charge even more does not provide any further advantage. The E protein mutations that were selected in this study were of the type that had already been observed in other studies with TBEVs (reviewed in reference 25) with normal monocistronic genome arrangements, and so these mutations were probably not involved in adaptation of the bicistronic virus per se but instead represent a general adaptation mechanism by which the E protein acquires a stronger binding affinity for BHK-21 cells.

In contrast, it is striking that the other mutations that were selected with TBEV-bc were within the foreign IRES element itself and that a very similar mutation in the IRES was also selected in a mouse and appeared to be associated with increased pathogenicity. Since all of these mutations decreased the functional efficiency of the IRES, it is reasonable to assume that they were selected because they were able to compensate for a deleterious effect of having the IRES and/or the prM and E genes inserted into that particular position in the 3′NCR. Because it is not yet clear which factors are limiting in the viral replication cycle, we do not know whether the resulting lowered rate of translation of prM and E was actually harmful to the virus in this case, but it can be presumed that another factor, such as RNA replication and/or efficiency of cap-dependent translation, was probably more important for the selection process. This interpretation is supported by the observation that all of the IRES mutations consistently restored expression of the proteins from the cap cistron to wild-type levels. This leads to the rather unexpected conclusion that enhancing RNA replication and translation of nonstructural proteins was a more important determinant for improving viral fitness than the level of surface protein (M and E) expression.

The functional organization of IRES elements has been extensively studied, and it is clear that the oligo(A) loop of the J-K stem-loop structure in the EMCV IRES, where mutations were found in this study, is an important functional element that is directly involved in the association of the IRES with the cellular translation machinery. Using primer extension analysis as well as chemical and enzymatic protection experiments, it has been shown that this region serves as a binding site for eIF4G (20, 21), and this ability to bind eIF4G directly is the key feature that makes IRES initiation independent of a 5′ cap structure (33). Mutations in the oligo(A) loop have been found to impair translation (13, 14), and the total number of A's in this loop is known to affect the strength of the IRES (2) as well as which cofactors are required for optimal efficiency (17).

Since the mutations that we selected in the bicistronic TBEV genome were of the type that apparently reduce the affinity of translation initiation factors for the inserted IRES, it can be speculated that these factors or, indirectly, the ribosome complexes that are recruited by these factors interfere with virus replication when bound tightly to the IRES, and this could account for our earlier observation that the level of TBEV-bc RNA replication is low compared to that of the normal monocistronic genome (32). This, for example, could lower the amount of free template RNA that is available to the flavivirus RNA replication machinery for the initiation of RNA synthesis. Furthermore, it has been observed with other positive-strand RNA viruses that when ribosomes, moving in the 5′-to-3′ direction during translation, collide with the viral replication machinery moving in the opposite direction during minus-strand synthesis, translation continues but RNA replication stops (1, 6). This implies that RNA replication can occur only when the RNA template is not monopolized by the translation machinery. A mutation that increases the initial rate of RNA replication at the expense of protein translation might therefore be particularly advantageous during the early stages of infection, especially if RNA template availability has become rate-limiting for the entire process. Indeed, preliminary data, obtained using a sensitive luciferase expression system, support the hypothesis that mutations in the oligo(A) loop of the IRES increase RNA replication efficiency (V. M. Hoenninger and C. W. Mandl, unpublished results). This phenomenon might also account for the apparent five- to sevenfold increase in specific infectivity imparted by the IRES-A771C mutation (Fig. 3C), because a long delay in the onset of RNA synthesis would increase the likelihood of the viral RNA being degraded in the cell before a productive infection can be established.

It is also possible that competition for ribosomes between the cap and IRES elements causes an imbalance at the translation level that results in suboptimal ratios of structural and nonstructural proteins synthesized from different cistrons. Although this, potentially, is a general problem of all bicistronic expression systems with interacting components, viral vector systems that depend on both cistrons for their replication would be expected to be especially sensitive in this respect. Currently, although it has been established that each flavivirus virion has 180 copies each of E and M (31), little is known otherwise about the required stoichiometry of the replication complexes or the nucleocapsid or the relative amounts of the different structural and nonstructural proteins that are required during the various stages of the replication cycle. In this context, it is interesting to note that the A771C mutation not only resulted in a seven- to ninefold increase in expression of the viral surface proteins (pr)M and E from the IRES but also resulted in a proportionally lower (twofold) increase in expression of the other viral protein from the cap cistron. This means that the mutation, although by itself impairing the functionality of the IRES, ultimately caused an increase in the ratio of IRES-translated prM/E dimers relative to the capsid protein and nonstructural proteins, which was probably beneficial for virus assembly. This paradoxical observation is difficult to explain unless one considers the combined effects of the mutation on RNA synthesis and translation. If weakening the IRES causes less interference with RNA replication, as discussed above, the resulting increase in the total number of RNA molecules, and thus the number of cap and IRES elements competing for translation factors, might ultimately tip the balance in favor of the stronger translation element, the IRES.

The acquisition of variable numbers of additional adenine insertions in the oligo(A) loop of the IRES appears to be another way in which the bicistronic TBEV can make further

compensatory adjustments in the level of function of the foreign IRES. Astonishingly, a mutant IRES with a total of 19A's in this loop was still functional, retaining 50% activity in the reporter construct, and even a 45-A loop mutant retained 16% activity. The TBEV-bc construct containing the 19-A loop was not significantly impaired in its ability to replicate and produce infectious particles (despite a lower efficiency of translation from the IRES), whereas mutants with even more A's (26 and 45) were less robust. If these larger insertions were actually selected in our experiments, it is not completely clear what advantage they provided, especially since the 45-A mutant was difficult to maintain in cell culture and the isolated 26-A variant continued to mutate, again producing a mixture of loop sizes. However, the somewhat different kinetics of envelope protein expression that these mutants display compared to TBEV-bc, as shown in Fig. 5D, might provide a clue. In these experiments, the amount of E protein in the cells was higher for the first 2 to 3 days after transfection with the poly(A) mutants than with the parental bicistronic virus, and this might have provided an opportunity for these mutants to gain an early, although temporary, advantage. Another likely interpretation of our findings is that the most viable (and thus selected for) sequence is represented by an oligo(A) loop which is increased by only a few A residues. However, this length may be above a threshold at which the viral replicase starts to have a high propensity to slip and slide and thus create the distribution of various loop lengths observed in our experiments. In this case, the longer A loops would actually represent less fit and aberrant by-products of replication, whereas shorter forms present in the mixture of RNA molecules would be mainly responsible for the increased viral fitness.

It is also interesting, and probably significant, that the variable region that was replaced by the IRES cistron in TBE-bc often contains an internal poly(A) tract of from 6 (41) to more than 200 (30) nucleotides. Because this region is highly variable in length, is completely lacking in some strains (30, 41), and can be removed from strains that do have it (28), it does not appear to have an essential function, but it is nevertheless possible that it provides a selective advantage in natural hosts, since it seems to appear more frequently in primary isolates and sometimes becomes deleted or shortened in strains that have undergone cell culture passage (28). The TBEV strain Neudoerfl, from which our construct was derived, has an internal poly(A) tract, and it is possible that insertions in the oligo(A) loop in the IRES serve to restore this element and, with it, whatever growth advantage that it provides.

In practical terms, this study has revealed two types of mutations that improve the efficiency of bicistronic flavivirus replication in an additive manner, and it also identifies potential targets for further improvements. Achieving the correct balance between the two translation units as well as the balance between translation and replication are key considerations in the development of artificial bicistronic viral expression systems.

ACKNOWLEDGMENTS

We are grateful to Steven L. Allison for many helpful discussions and for his invaluable assistance during data evaluation and preparation of the manuscript. We also thank Gabriela Perstinger and Ursula Sinzinger for technical help with FACS analysis.

This project was funded in part by two grants from the Austrian "Fonds zur Förderung der wissenschaftlichen Forschung" (FWF project numbers P16376-B04 and P17584-B14).

REFERENCES

1. **Barton, D. J., B. J. Morasco, and J. B. Flanegan.** 1999. Translating ribosomes inhibit poliovirus negative-strand RNA synthesis. J. Virol. **73:**10104–10112.
2. **Bochkov, Y. A., and A. C. Palmenberg.** 2006. Translational efficiency of EMCV IRES in bicistronic vectors is dependent upon IRES sequence and gene location. BioTechniques **41:**283–288.
3. **Domingo, E., C. Escarmis, N. Sevilla, A. Moya, S. F. Elena, J. Quer, I. S. Novella, and J. J. Holland.** 1996. Basic concepts in RNA virus evolution. FASEB J. **10:**859–864.
4. **Drake, J. W., B. Charlesworth, D. Charlesworth, and J. F. Crow.** 1998. Rates of spontaneous mutation. Genetics **148:**1667–1686.
5. **Elshuber, S., S. L. Allison, F. X. Heinz, and C. W. Mandl.** 2003. Cleavage of protein prM is necessary for infection of BHK-21 cells by tick-borne encephalitis virus. J. Gen. Virol. **84:**183–191.
6. **Gamarnik, A. V., and R. Andino.** 1998. Switch from translation to RNA replication in a positive-stranded RNA virus. Genes Dev. **12:**2293–2304.
7. **Gehrke, R., F. X. Heinz, N. L. Davis, and C. W. Mandl.** 2005. Heterologous gene expression by infectious and replicon vectors derived from tick-borne encephalitis virus and direct comparison of this flavivirus system with an alphavirus replicon. J. Gen. Virol. **86:**1045–1053.
8. **Germi, R., J. M. Crance, D. Garin, J. Guimet, H. Lortat-Jacob, R. W. Ruigrok, J. P. Zarski, and E. Drouet.** 2002. Heparan sulfate-mediated binding of infectious dengue virus type 2 and yellow fever virus. Virology **292:** 162–168.
9. **Goto, A., D. Hayasaka, K. Yoshii, T. Mizutani, H. Kariwa, and I. Takashima.** 2003. A BHK-21 cell culture-adapted tick-borne encephalitis virus mutant is attenuated for neuroinvasiveness. Vaccine **21:**4043–4051.
10. **Hayasaka, D., K. Yoshii, T. Ueki, T. Iwasaki, and I. Takashima.** 2004. Sub-genomic replicons of tick-borne encephalitis virus. Arch. Virol. **149:** 1245–1256.
11. **Heinz, F. X., W. Tuma, F. Guirakhoo, and C. Kunz.** 1986. A model study of the use of monoclonal antibodies in capture enzyme immunoassays for antigen quantification exploiting the epitope map of tick-borne encephalitis virus. J. Biol Stand. **14:**133–141.
12. **Hellen, C. U., and E. Wimmer.** 1995. Translation of encephalomyocarditis virus RNA by internal ribosomal entry. Curr. Top. Microbiol. Immunol. **203:**31–63.
13. **Hoffman, M. A., and A. C. Palmenberg.** 1995. Mutational analysis of the J-K stem-loop region of the encephalomyocarditis virus IRES. J. Virol. **69:**4399–4406.
14. **Hoffman, M. A., and A. C. Palmenberg.** 1996. Revertant analysis of J-K mutations in the encephalomyocarditis virus internal ribosomal entry site detects an altered leader protein. J. Virol. **70:**6425–6430.
15. **Iacono-Connors, L. C., J. F. Smith, T. G. Ksiazek, C. L. Kelley, and C. S. Schmaljohn.** 1996. Characterization of Langat virus antigenic determinants defined by monoclonal antibodies to E, NS1 and preM and identification of a protective, non-neutralizing preM-specific monoclonal antibody. Virus Res. **43:**125–136.
16. **Jones, C. T., C. G. Patkar, and R. J. Kuhn.** 2005. Construction and applications of yellow fever virus replicons. Virology **331:**247–259.
17. **Kaminski, A., G. J. Belsham, and R. J. Jackson.** 1994. Translation of encephalomyocarditis virus RNA: parameters influencing the selection of the internal initiation site. EMBO J. **13:**1673–1681.
18. **Khromykh, A. A., and E. G. Westaway.** 1997. Subgenomic replicons of the flavivirus Kunjin: construction and applications. J. Virol. **71:**1497–1505.
19. **Kofler, R. M., V. M. Hoenninger, C. Thurner, and C. W. Mandl.** 2006. Functional analysis of the tick-borne encephalitis virus cyclization elements indicates major differences between mosquito-borne and tick-borne flaviviruses. J. Virol. **80:**4099–4113.
20. **Kolupaeva, V. G., I. B. Lomakin, T. V. Pestova, and C. U. Hellen.** 2003. Eukaryotic initiation factors 4G and 4A mediate conformational changes downstream of the initiation codon of the encephalomyocarditis virus internal ribosomal entry site. Mol. Cell. Biol. **23:**687–698.
21. **Kolupaeva, V. G., T. V. Pestova, C. U. Hellen, and I. N. Shatsky.** 1998. Translation eukaryotic initiation factor 4G recognizes a specific structural element within the internal ribosome entry site of encephalomyocarditis virus RNA. J. Biol. Chem. **273:**18599–18604.
22. **Kroschewski, H., S. L. Allison, F. X. Heinz, and C. W. Mandl.** 2003. Role of heparan sulfate for attachment and entry of tick-borne encephalitis virus. Virology **308:**92–100.
23. **Lindenbach, B. D., and C. M. Rice.** 2001. Flaviviridae: the viruses and their replication, p. 991–1041. *In* D. M. Knipe and P. M. Howley (ed.), Fields virology, 4th ed. Lippincott Williams & Wilkins, Philadelphia, PA.
24. **Lo, M. K., M. Tilgner, and P. Y. Shi.** 2003. Potential high-throughput assay for screening inhibitors of West Nile virus replication. J. Virol. **77:**12901–12906.
25. **Mandl, C. W.** 2005. Steps of the tick-borne encephalitis virus replication cycle that affect neuropathogenesis. Virus Res. **111:**161–174.

26. **Mandl, C. W., S. L. Allison, H. Holzmann, T. Meixner, and F. X. Heinz.** 2000. Attenuation of tick-borne encephalitis virus by structure-based site-specific mutagenesis of a putative flavivirus receptor binding site. J. Virol. **74:**9601–9609.
27. **Mandl, C. W., M. Ecker, H. Holzmann, C. Kunz, and F. X. Heinz.** 1997. Infectious cDNA clones of tick-borne encephalitis virus European subtype prototypic strain Neudoerfl and high virulence strain Hypr. J. Gen. Virol. **78:**1049–1057.
28. **Mandl, C. W., H. Holzmann, T. Meixner, S. Rauscher, P. F. Stadler, S. L. Allison, and F. X. Heinz.** 1998. Spontaneous and engineered deletions in the 3′ noncoding region of tick-borne encephalitis virus: construction of highly attenuated mutants of a flavivirus. J. Virol. **72:**2132–2140.
29. **Mandl, C. W., H. Kroschewski, S. L. Allison, R. Kofler, H. Holzmann, T. Meixner, and F. X. Heinz.** 2001. Adaptation of tick-borne encephalitis virus to BHK-21 cells results in the formation of multiple heparan sulfate binding sites in the envelope protein and attenuation in vivo. J. Virol. **75:**5627–5637.
30. **Mandl, C. W., C. Kunz, and F. X. Heinz.** 1991. Presence of poly(A) in a flavivirus: significant differences between the 3′ noncoding regions of the genomic RNAs of tick-borne encephalitis virus strains. J. Virol. **65:**4070–4077.
31. **Mukhopadhyay, S., R. J. Kuhn, and M. G. Rossmann.** 2005. A structural perspective of the flavivirus life cycle. Nat. Rev. Microbiol. **3:**13–22.
32. **Orlinger, K. K., V. M. Hoenninger, R. M. Kofler, and C. W. Mandl.** 2006. Construction and mutagenesis of an artificial bicistronic tick-borne encephalitis virus genome reveals an essential function of the second transmembrane region of protein e in flavivirus assembly. J. Virol. **80:**12197–12208.
33. **Pestova, T. V., I. N. Shatsky, and C. U. Hellen.** 1996. Functional dissection of eukaryotic initiation factor 4F: the 4A subunit and the central domain of the 4G subunit are sufficient to mediate internal entry of 43S preinitiation complexes. Mol. Cell. Biol. **16:**6870–6878.
34. **Puig-Basagoiti, F., T. S. Deas, P. Ren, M. Tilgner, D. M. Ferguson, and P. Y. Shi.** 2005. High-throughput assays using a luciferase-expressing replicon, virus-like particles, and full-length virus for West Nile virus drug discovery. Antimicrob. Agents Chemother. **49:**4980–4988.
35. **Ruggli, N., and C. M. Rice.** 1999. Functional cDNA clones of the Flaviviridae: strategies and applications. Adv. Virus Res. **53:**183–207.
36. **Scholle, F., Y. A. Girard, Q. Zhao, S. Higgs, and P. W. Mason.** 2004. *trans*-packaged West Nile virus-like particles: infectious properties in vitro and in infected mosquito vectors. J. Virol. **78:**11605–11614.
37. **Shi, P. Y., M. Tilgner, and M. K. Lo.** 2002. Construction and characterization of subgenomic replicons of New York strain of West Nile virus. Virology **296:**219–233.
38. **Stadler, K., S. L. Allison, J. Schalich, and F. X. Heinz.** 1997. Proteolytic activation of tick-borne encephalitis virus by furin. J. Virol. **71:**8475–8481.
39. **Varnavski, A. N., and A. A. Khromykh.** 1999. Noncytopathic flavivirus replicon RNA-based system for expression and delivery of heterologous genes. Virology **255:**366–375.
40. **Varnavski, A. N., P. R. Young, and A. A. Khromykh.** 2000. Stable high-level expression of heterologous genes in vitro and in vivo by noncytopathic DNA-based Kunjin virus replicon vectors. J. Virol. **74:**4394–43403.
41. **Wallner, G., C. W. Mandl, C. Kunz, and F. X. Heinz.** 1995. The flavivirus 3′-noncoding region: extensive size heterogeneity independent of evolutionary relationships among strains of tick-borne encephalitis virus. Virology **213:**169–178.
42. **Wengler, G., and G. Wengler.** 1981. Terminal sequences of the genome and replicative-form RNA of the flavivirus West Nile virus: absence of poly(A) and possible role in RNA replication. Virology **113:**544–555.
43. **Wengler, G., G. Wengler, and H. J. Gross.** 1978. Studies on virus-specific nucleic acids synthesized in vertebrate and mosquito cells infected with flaviviruses. Virology **89:**423–437.
44. **Yoshii, K., D. Hayasaka, A. Goto, K. Kawakami, H. Kariwa, and I. Takashima.** 2005. Packaging the replicon RNA of the Far-Eastern subtype of tick-borne encephalitis virus into single-round infectious particles: development of a heterologous gene delivery system. Vaccine **23:**3946–3956.
45. **Zuker, M.** 2003. Mfold web server for nucleic acid folding and hybridization prediction. Nucleic Acids Res. **31:**3406–3415.